4.5 Damping Ring

4.5.1 Introduction

In a first design of a damping ring for the SBLC [1] the FODO, Inverse-Bending-Cells and the Chasman-Green lattices were investigated. The Chasman-Green lattice has been chosen, because its dynamic aperture was two to three times higher than for the other structures. For a storage ring built of 72 identical cells the acceptance is 42 mm mrad, not taking into account magnet errors.

In order to meet the strict requirements on the damping time, damping wigglers have to be introduced in the storage ring. Conventionally, the ring is replaced by a racetrack structure: two arcs with bends and two long straight sections that accommodate the damping wigglers, injection, extraction and the RF-system. In such a scheme the dynamic aperture is drastically reduced. In the design of [1] the length of the straight section was around 80 m and the acceptance dropped from 42 to 6.5 mm mrad.

The damping rings for the ATF-damping-test-facility [2] and the NLC-project [3] are also racetrack in shape. But there the arcs are based on the TME (Theoretical Minimum Emittance) [4] lattice, which results in a smaller emittance. The application of a TME-lattice to a storage ring has been done first for Super-ACO [5] and recently proposed for a low-emittance synchrotron light source [6, 7, 8].

In a recent design [9] for a 300 m damping ring for the SBLC project we found that the reduction of the dynamic aperture is less drastic when the damping wigglers are distributed around the ring. The requirements concerning the emittance and the damping time could be fulfilled with a TBA-lattice [10] whose straight sections are occupied by damping wigglers.

Furthermore, the radiation power of a wiggler with a length of 5 m (E = 3 GeV, I = 0.3 A) is in the same order as that of the ESRF-Wigglers. Hence the handling of such a power can be done.

In this section we present a re-design of the damping ring which profits from the larger dynamic aperture of a lattice with distributed wigglers. The proposed design is based upon the ESRF-synchrotron-light source [11].

4.5.2 Damping Ring Requirements

The requirements for the damping ring are given by the parameters of the SBLC (Section 4.1) and the specification of the injection system (Section 4.4). The time structure of the SBLC, relevant for the damping ring design, is presented in figure 4.5.1.

The emittance of the beam from the pre-accelerator is 10^{-4} m for electrons and 10^{-3} to 10^{-2} m for positrons. According to the parameters, the damping ring has to reduce the emittance within a time of 20 ms down to $4 \cdot 10^{-6}$ m horizontally and $2 \cdot 10^{-7}$ m vertically. Here, an emittance dilution budget of 25 % from the damping ring to the IP is taken into account. Having a pulse length of 2μs, the circumference of the damping ring has to be more than 600 m.

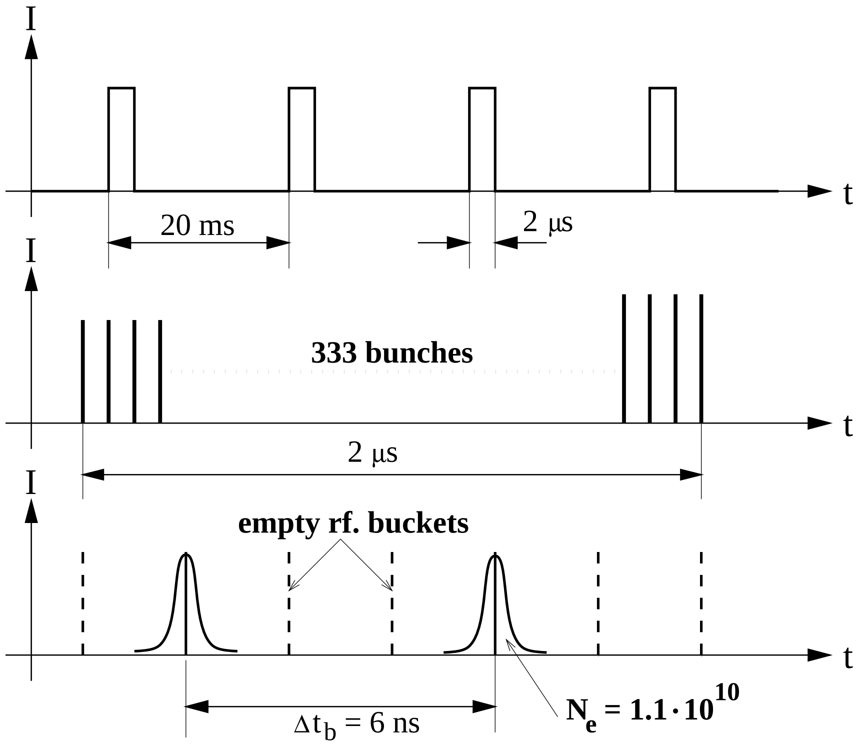

Figure 4.5.1: *Time structure of the SBLC (f_{rep} = 50 Hz, $t_{puls} = 2\,\mu s$, Δt_{puls} = 6 ns, f_{RF} = 500 MHz for the ring RF-system).*

The damping of the emittance within a storage ring is:

$$\varepsilon_f = \varepsilon_{inj} \cdot e^{-2N_\tau} + \varepsilon_{equ} \cdot (1 - e^{-2N_\tau}) \tag{4.5.1}$$

where ε_{inj} is the emittance of the injected beam and ε_{equ} is the equilibrium emittance of the damping ring. N_τ is the number of damping times the beam has been stored, i.e. $N_\tau = t/\tau_D$, where τ_D is the damping time.

From eq. (4.5.1) follows the necessary equilibrium emittance ε_{equ} at a given accumulation time t:

$$\varepsilon_{equ} = \frac{\varepsilon_f - \varepsilon_{inj} \cdot e^{-2 \cdot t/\tau_D}}{1 - e^{-2 \cdot t/\tau_D}} \tag{4.5.2}$$

The required vertical damping times for the different injection emittances are given in table 4.5.2. The requirements for the horizontal plane are more relaxed: $N_{\tau_x} = 1.5$ and $\tau_x = 13.1$ ms.

The equilibrium emittance ε_{equ} in the vertical direction as a function of the damping time τ_D with is presented in figure 4.5.2 for the the injection emittances $1 \cdot 10^{-2}$ m and $5 \cdot 10^{-3}$ m respectively. The vertical equilibrium emittance is determined by the alignment tolerances and the correction procedures (see below). At 3rd generation light sources coupling factors of less than 1 % are normal. With an emittance in the x- direction of $4 \cdot 10^{-6}$ m and a coupling factor of 2 %, the vertical emittance will be

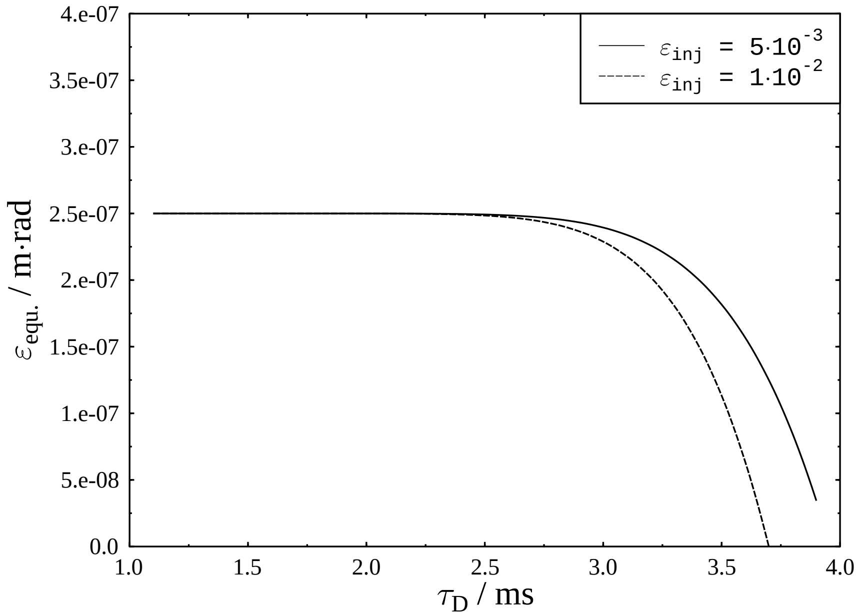

Figure 4.5.2: *The equilibrium emittance in the vertical direction as a function of the damping time* τ_D. $\varepsilon_f = 2 \cdot 10^{-7}$ $m \cdot rad$, $t = 20\,ms$ *and* $\varepsilon_{inj} = 1 \cdot 10^{-2}$ *and* $5 \cdot 10^{-3}\,m$ *respectively. The final emittance* $\varepsilon_f = 2 \cdot 10^{-7}\,m$.

$1 \cdot 10^{-7}$ m. In order to meet the requirements for the SBLC-DR, the damping time must be smaller than 3.5 ms.

ε_{inj} $m \cdot rad$	N_{τ_y}	τ_y ms	Remarks
$1 \cdot 10^{-2}$	5.60	3.50	Positrons
$1 \cdot 10^{-3}$	4.45	4.40	Positrons
$1 \cdot 10^{-4}$	3.17	6.00	Electrons

Table 4.5.1: *Required vertical damping time* τ_y *for the SBLC damping ring for a storage time of 20 ms and a final emittance* $\varepsilon_{y,n}$ *of* $2 \cdot 10^{-7}$ *m.*

We thus adopt the following requirements for the damping ring:

$$\varepsilon_{x,n} \leq 4 \cdot 10^{-6} m \ , \ \varepsilon_{y,n} \leq 10^{-7} m \qquad and \qquad \tau_y \leq 3.5 ms. \tag{4.5.3}$$

The energy of the damping ring should be in the range between 2.5 and 3.5 GeV. At an energy of 3 GeV the normalized emittance of $4 \cdot 10^{-6}$ m translates into an absolute horizontal emittance of $6.7 \cdot 10^{-10}$ m which is in the domain of a fourth generation light source [12], about an order of magnitude below existing third generation light sources [13].

The damping time of a storage ring without any insertion devices is given by:

$$\tau_i = \frac{[C/m] \cdot [\rho/m]}{13.2 \cdot J_i \cdot [E/GeV]^3} ms \tag{4.5.4}$$

with C the circumference, ρ the curvature of the bending magnets, J_i the partition number for the corresponding mode and E the energy of the beam. With the circumference and energy fixed to 600 m and 3 GeV, respectively, and the highest reasonable magnetic flux of 1.5 T, the lowest possible vertical damping time becomes 12 ms. A further reduction can be done only with damping wigglers which, on the other hand, influence also the emittance [14, 15]. By a proper design of the wigglers, however, the equilibrium emittance may be lower, too.

4.5.3 Lattice of the Damping Ring

In principle the requirements set on the damping ring can be met with a racetrack design, as already proposed for the other linear collider projects. However, another variable to consider is the dynamic aperture which has to accommodate the required beam current. Based on our investigations for a fourth generation synchrotron light source [16] we propose to adopt a design with a distributed wiggler arrangement similar to a light source, with the places for insertion devices occupied solely by damping wigglers.

The design of - existing or proposed - light sources are based on different lattice structures: FODO, DBA, TBA and TME [13]. Their emittances scale by the following law:

$$\varepsilon = C_q \cdot \gamma^2 \cdot \frac{1}{J_x} \cdot K \cdot \frac{1}{12\sqrt{15}} \cdot \varphi^3 \tag{4.5.5}$$

with the constant $C_q = 3.84 \cdot 10^{-13}$, and the variables: γ the Lorentz factor, φ the deflection angle of the bending magnet, J_x the horizontal partition number, and K the quality factor of the lattice. The quality factor as it is defined through eq. (4.5.5) is implicitly a measure for how compact a machine can reach a given emittance. The K-values for different optics are summarised in table 3. The DBA lattice has the lowest K value achieved in practice.

Because damping wigglers have to be introduced, one should also consider how much space for insertion devices are available with different optics. The DBA has the most space, which has been shown in an investigation by Wrulich [17].

According to both arguments above, we have chosen a DBA lattice based on the ESRF design [11] as the best candidate for the damping ring lattice. The lattice functions within a unit cell of our SBLC damping ring design are given in Fig. 4.5.3a and in Table 4.5.3 the parameters of the ring are compared to those of the ESRF. The machine functions within a unit cell including the damping wiggler are presented in

Optic	K/theoretic	K/real	Machines
FODO	58	2000	PETRA
DBA	3	6.3	ESRF
		4.6	ELETTRA
TBA	2.33	13	BESSY I
		11	ALS
TME	1	-	-

Table 4.5.2: *The quality factor K for different optics.*

Fig. 4.5.3b. As a result of the focusing of the wigglers in the vertical direction the shape of the vertical betatron functions looks differently by installing a wiggler in the straight section. The betatron functions in Fig. 4.5.3 have been matched to the same working points $Q_x = 30.18$, $Q_y = 10.24$, respectively, with and without wigglers.

	ESRF	SBLC-DR
Energy (GeV)	6	3
Beam current (mA)	200	300
Magnet bending radius (m)	24.9555	13.5427
Bending field (T)	0.802	0.7389
Deflection angle per magnet	5.625	5.000
Circumference (m)	844.4	660
Number of super periods	16	36
Horizontal working point Q_x	36.2	30.18
vertical working point Q_y	11.2	10.24
Momentum compaction factor	$3.1 \cdot 10^{-4}$	$1.64 \cdot 10^{-4}$
Synchrotron damping time (ms)	3.7	12.4
Horizontal damping time (ms)	7.4	24.8
Vertical damping time (ms)	7.4	24.8
Horizontal emittance (nm rad)	6.20	3.2
Vertical emittance (nm rad)	0.62	0.32
Horizontal chromaticity	-113.9	-48.8
Vertical chromaticity	-34.50	-31.5
Energy spread (σ_E/E)	$1.03 \cdot 10^{-3}$	$0.7 \cdot 10^{-3}$

Table 4.5.3: *Comparison of the main parameters of the SBLC damping ring with the ESRF design.*

As given by eq. (4.5.4) the damping time is determined by the circumference, the radius of curvature and the energy. To reach a small damping time at a fixed circumference, the radius should be as small as possible. The radius of curvature also influences the emittance and the momentum compaction factor α: ε is proportional to

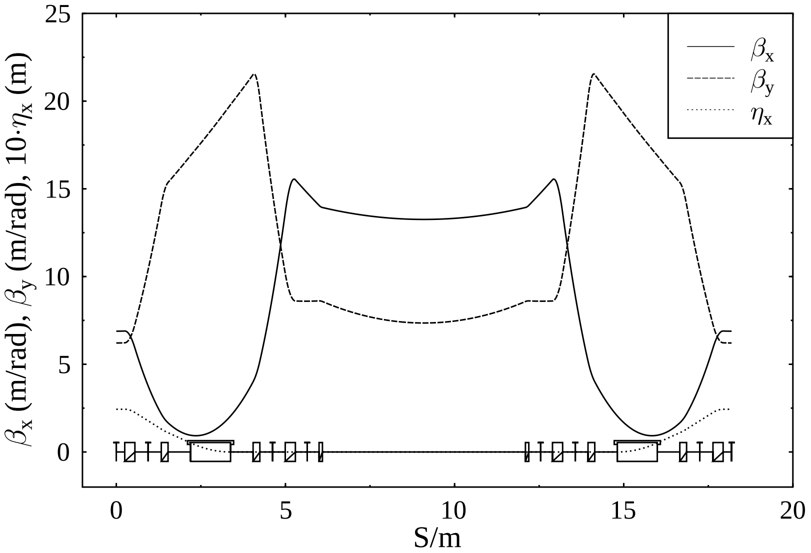

(a) (b)

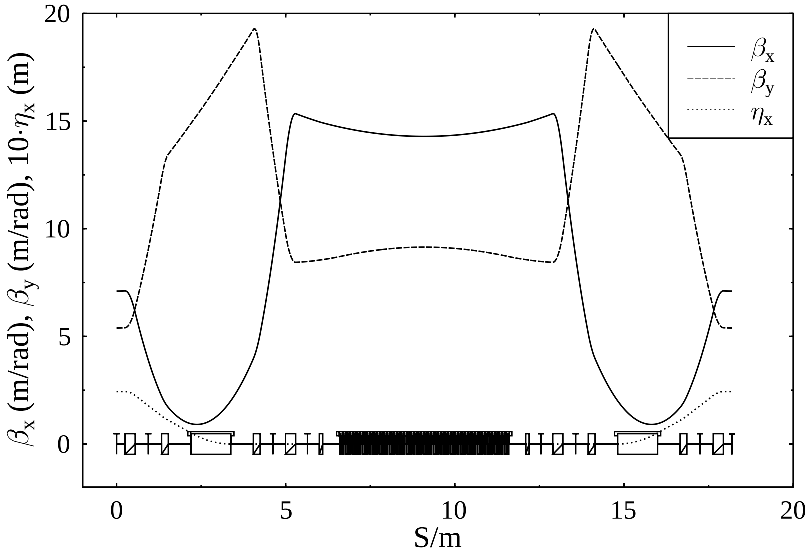

Figure 4.5.3: *The lattice functions within a unit cell of the proposed SBLC damping ring. The deflection angle per magnet is 5 degrees and the periodicity is 36. (a) the bare DBA-cell and (b) half of the DBA-structure with a damping wiggler in the straight section.*

$1/\rho$ (eq. (4.5.5)) and α is proportional to ρ. The momentum compaction factor of a DBA lattice is given by:

$$\alpha[DBA] = \frac{\rho \cdot N_M}{C}\{2 \cdot \pi \cdot \frac{\varphi}{360} - \sin\varphi\} \tag{4.5.6}$$

with N_M is the number of bending magnets of the ring and φ the deflection angle of each bending magnet in degrees. Due to the larger bending radius of the ESRF, its α is approximately 2 times higher than the SBLC-damping ring. All other factors of the two designs are more or less in the same range.

The dynamic aperture of the bare ring (without damping wigglers) is given in Fig. 4.5.4. The corresponding acceptances are 128 mm mrad horizontally and 100 mm mrad vertically. Although the dispersion function of the SBLC-damping ring is smaller than for the ESRF-ring which leads to higher sextupole strengths, the dynamic aperture is larger. The calculations for the dynamic aperture have been performed with the codes MAD [19], RACETRACK [20] and BETA [21]. The results of all three codes are in good agreement (better than $\pm 10\%$).

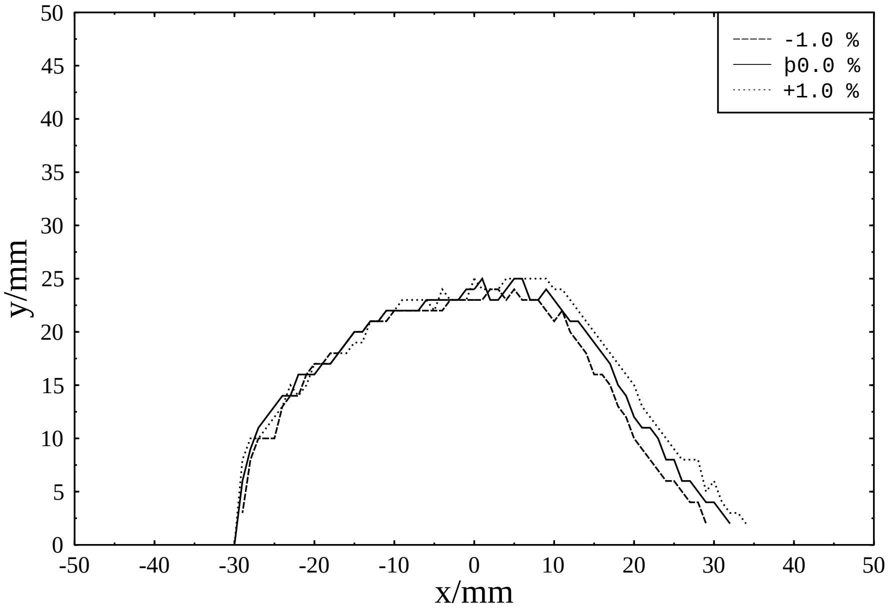

Figure 4.5.4: *The dynamic aperture of the bare SBLC damping ring including harmonic sextupoles. These values have been calculated with the code MAD.*

The shifts of the tune with energy and betatron amplitude are presented in Fig. 4.5.5 and Fig. 4.5.6, respectively.

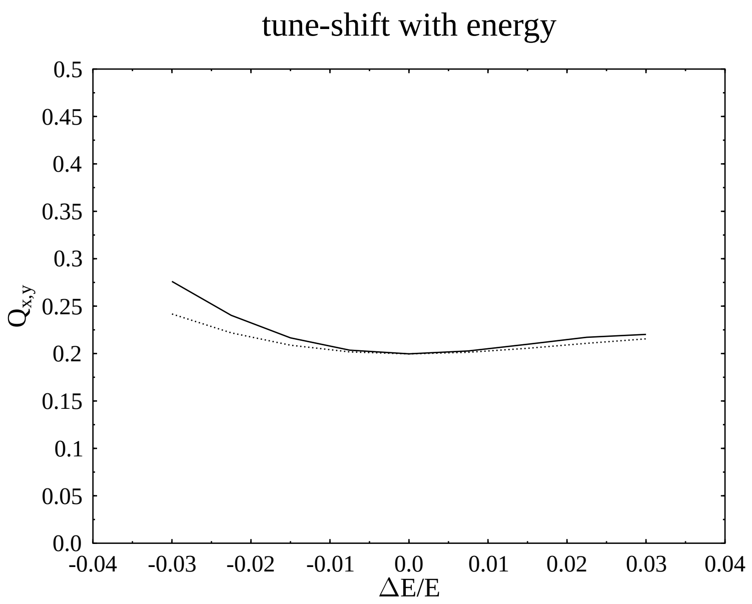

Figure 4.5.5: *Tune shift with energy of the bare damping ring according to figure 4.5.3, above. Without any errors.*

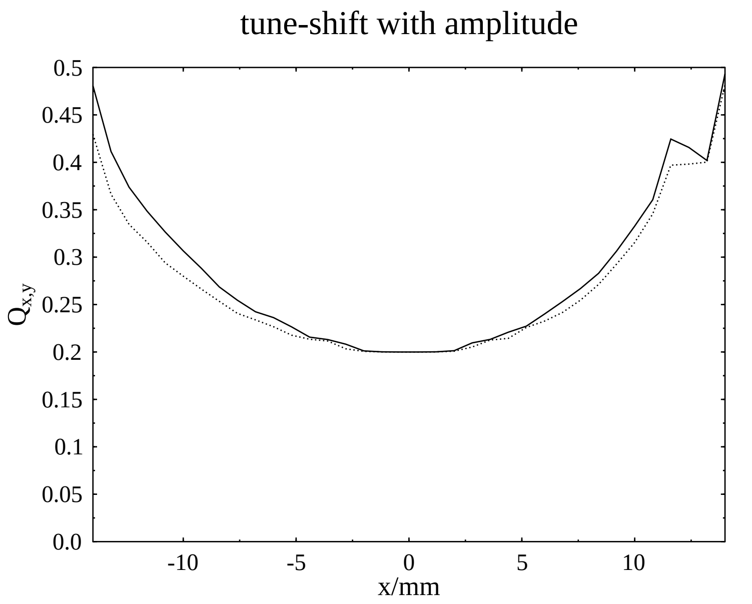

Figure 4.5.6: *Tune shift with amplitude of the bare damping ring as determined by the optics of figure 4.5.3a. No errors have been taken into account.*

The calculations of the tune shift with the energy deviations have been done in the range of $\pm 3\,\%$. From Fig. 4.5.5 one can conclude that the energy acceptance of the bare lattice is larger than $\pm 4\,\%$ which is more than sufficient.

With increasing amplitudes of the betatron oscillations the tunes are moving in the directions of the half order resonances, which determines the dynamic aperture too. With the amplitudes of figure 4.5.6 the working point crosses only the resonance line $Q_x + 4 \cdot Q_y = 2 \cdot 36$ which is a harmless one.

The maximum amplitudes in figure 4.5.6 are smaller than in figure 4.5.4 for the dynamic aperture. The reason is because for the calculation of the tune shift a combined effec from the x and y direction exists. Taking this into account the results shown in Figs. 4.5.4 and 4.5.6 are compatible.

4.5.4 Introduction of Wigglers

The wigglers have an effect on the damping time, the energy spread and the emittance. The relations [14, 15] are given in Table 4.5.4.

4.5.4.1 Effect on the Emittance

The SBLC damping ring has 36 straight sections. Six are needed for injection, extraction and the RF system. The length of a straight section - from quadrupole to quadrupole - is 6 m. Therefore, the length of one wiggler could be around 5 m, resulting in an overall length of 150 m of installed wigglers. The maximum magnetic field of a wiggler is 2 T leading to a minimum radius of curvature of 5 m. The period length of the wigglers has been set to 0.2 m. With these values, the emittance is according to Table 4.5.4:

$$\begin{aligned} \varepsilon_{x,wi} &= \varepsilon_{x,0} \cdot 0.202 = 6.5 \cdot 10^{-10} mrad \\ \varepsilon_{x,n} &= \gamma \cdot \varepsilon_{x,wi} = 3.8 \cdot 10^{-6} mrad \end{aligned} \tag{4.5.7}$$

The contribution of the term I_5^{ID}/I_5^0 is roughly 34 %. Hence a reduction of the emittance can be achieved by altering the period length of the wiggler, the β- value in the middle of the straight section or the magnetic flux in the wiggler, as is demonstrated in the following examples:

By changing the period length to 0.175 m, the emittance is reduced to $3.5 \cdot 10^{-6}$mrad.

In our special case the emittance scales with the β- value in the middle of the straight section as:

$$\varepsilon \beta^{-0.335} = const \tag{4.5.8}$$

which means that by reducing β from 14.0 m to 7.0 m the normalised emittance becomes $3.0 \cdot 10^{-6}$ m.

The emittance as a function of the radius of curvature in the wigglers is shown in Fig. 4.5.7. This curve runs through a minimum at a curvature of $\rho_{wi} = 5$ m, which was chosen for the wiggler.

Table 4.5.4: *Effects of the wigglers on the damping time, emittance and energy spread*

$$\tau_{wi} = \tau_0 \cdot \frac{1}{1+(L_{ID} \cdot \rho_0/4\pi\rho_{wi}^2)}$$

$$\varepsilon_{x,wi} = \varepsilon_{x,0} \cdot \frac{1+[I_5^{ID}/I_5^0]}{1+[(I_2^{ID}-I_4^{ID})/(I_2^0-I_4^0)]}$$

$$\sigma_{E,wi}^2 = \sigma_{E,0}^2 \cdot \frac{1+[I_3^{ID}/I_3^0]}{1+[(2I_2^{ID}-I_4^{ID})/(2I_2^0-I_4^0)]}$$

$I_1^0 \cdots I_5^0$ are the well known synchrotron integrals,
$I_1^{ID} \cdots I_5^{ID}$ are the contributions of these integrals by the wigglers.
These integrals are given by [16],[17]

$$I_2^{ID} = L_{wi}/(2\rho_{wi}^2)$$

$$I_3^{ID} = 4 \cdot L_{wi}/(3 \cdot \pi\rho_{wi}^2)$$

$$I_4^{ID} = -(3 \cdot L_{wi} \cdot \lambda_{wi}^2/(32 \cdot \pi^2\rho_{wi}^4)$$

$$I_5^{ID} = I_5^{ID}(\langle\gamma\rangle) + I_5^{ID}(\langle\alpha\rangle) + I_5^{ID}(\langle\beta\rangle)$$

$$I_5^{ID}(\langle\gamma\rangle) = \frac{\lambda_{wi}^4 \cdot L_{ID}}{40\pi^2\rho_{wi}^5}\left(\frac{3}{5\pi} + \frac{3}{16}\right) \cdot \langle\gamma\rangle$$

$$I_5^{ID}(\langle\alpha\rangle) = -\frac{9 \cdot \lambda_{wi}^3 \cdot L_{ID}}{40\pi^4\rho_{wi}^5} \cdot \langle\alpha\rangle$$

$$I_5^{ID}(\langle\beta\rangle) = \frac{\lambda_{wi}^2 \cdot L_{ID}}{15\pi^3\rho_{wi}^5} \cdot \langle\beta\rangle$$

In a straight section of length l_0 and with the initial values
β_0, α_0 and γ_0 one gets the values:

$$\beta(s) = \beta_0 + \frac{s^2}{\beta_0},\ \alpha(s) = -\frac{s}{\beta_0},\ \gamma(s) = \frac{1}{\beta_0}$$

$$\langle\beta(s)\rangle = \beta_0 + \frac{1}{9} \cdot \frac{l_0^3}{\beta_0}$$
$$\langle\alpha(s)\rangle = -\frac{1}{2} \cdot \frac{l_0^2}{\beta_0}$$
$$\langle\gamma(s)\rangle = \frac{1}{\beta_0}$$

From the evaluation of the different contribution it follows that
$I_5^{ID}(\langle\gamma\rangle)$ and $I_5^{ID}(\langle\alpha\rangle) \ll I_5^{ID}(\langle\beta\rangle)$. Hence $I_5^{ID}(\langle\alpha\rangle)$ and $I_5^{ID}(\langle\gamma\rangle)$ can be neglected.

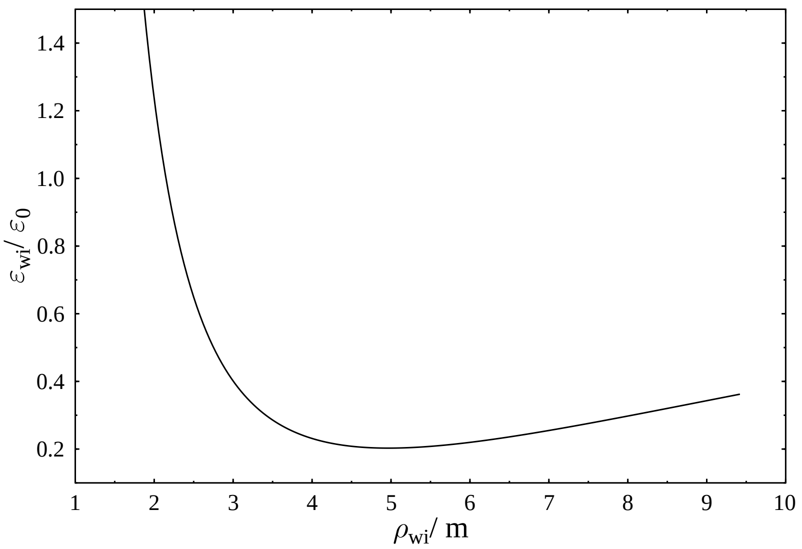

Figure 4.5.7: *Dependency of the emittance on the radius of curvature in the wiggler.*

In summary, by changing the period length from 0.2 to 0.175 m and reducing the β-value in the centre of the straight section from 14.0 m to 7 m a factor of 1.34 in the emittance can be gained.

4.5.4.2 Effect on the Damping Time

The damping time τ_i as function of the Energy E_0, the revolution time T_0, the partition function J_i and the radiation loss U per turn is as:

$$\tau_i = 2 \cdot \frac{E_0 \cdot T_0}{J_i \cdot U} \tag{4.5.9}$$

U on the other hand is determined by the radius ρ_0 of the bendings, the overall length L_{ID} of the wigglers and the curvature ρ_{wi} in the wigglers:

$$U = C_q \cdot \frac{E^4}{\rho_0} \{1 + \frac{L_{ID} \cdot \rho_0}{4\pi\rho_{wi}^2}\} \tag{4.5.10}$$

Combining these equations the damping time results in:

$$\tau_{wi} = 49.75ms \cdot \frac{[\rho_0/m]}{J_i \cdot [E_0/GeV]^3 \{1 + \frac{\rho_0}{\rho_w} \cdot \frac{L_{ID}}{4\pi\rho_w}\}} \tag{4.5.11}$$

which is visualised in Fig. 4.5.8 .

According to Fig. 4.5.8 the damping time can be decrease by reducing any or both of the radii of curvature. In our special case the damping time including wigglers scales with the radius of the bendings as well as the wigglers like

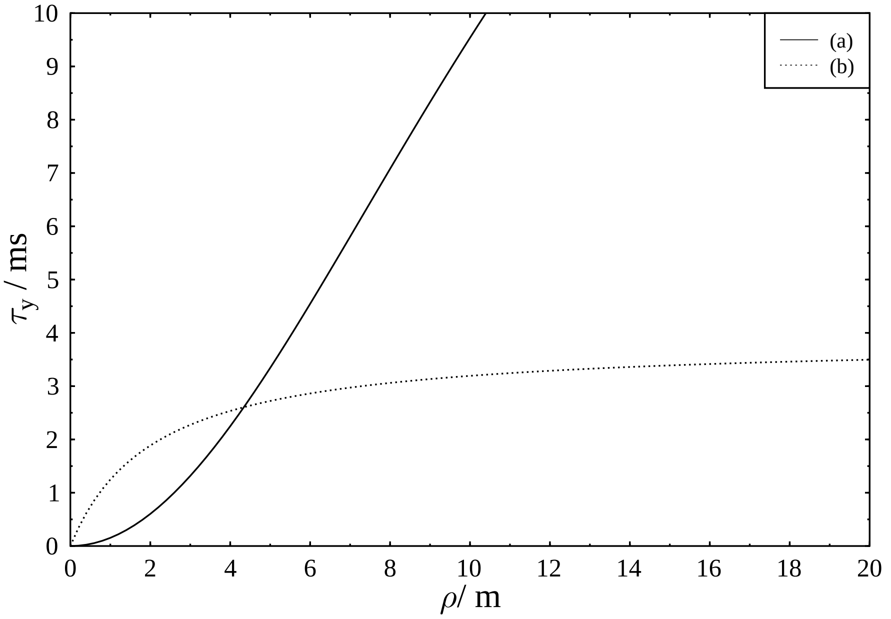

Figure 4.5.8: *The damping time as function of ρ_0 with $\rho_{wi} = 5m$ (b) and as a function of ρ_{wi} with $\rho_0 = 13.54$ (a).*

$$\tau_y \cdot \rho_{Bend}^{-0.14} = const \qquad \text{and} \qquad \tau_y \cdot \rho_{wi}^{-1.65} = const \tag{4.5.12}$$

According to eq. (4.5.12) the most effective way for changing the damping time is the variation of ρ_{wi}.

By keeping the radius of the bending magnet as well as the magnetic flux in the wigglers constant and alternating the energy of the electrons the damping time shows in comparison with eq. (4.5.4) only a small variation with the energy:

$$\tau_y \cdot E^{1.25} = const \tag{4.5.13}$$

The most effective way to change the damping time, without significantly changing the emittance, is to vary the radius of curvature of the wiggler and the beam energy.

For the SBLC damping ring the chosen parameters (B_w = 2 T, ρ_w = 5.0 m, λ_w = 0.2 m, E = 3 GeV, ρ_0 = 13.54 m) result in a damping time τ_y = 3.34 ms which fulfills the requirements.

In summary it may be stressed that the proposed SBLC-DR design with emittance ε_x of $3.8 \cdot 10^{-6}$ ms and damping time τ_y of 3.34 ms meets the requirements ($\varepsilon_x \leq 4 \cdot 10^{-6}$ m·rad and $\tau_y \leq 3.4$ ms).

4.5.4.3 Effect on the Energy Spread

The installation of the damping wigglers has an effect on the energy spread too (see table 4.5.4). Because I_2^{ID} and I_3^{ID} are larger than I_2^0 and I_3^0 the energy spread increases. With the values: $I_2^0 = 0.464$, $I_3^0 = 0.0343$, $I_2^{ID} = 3$ and $I_3^{ID} = 2.546$ the energy spread increases by a factor of 3.18 to $\frac{\sigma_E}{E} = 2.2 \cdot 10^{-3}$.

4.5.5 RF System

The layout of the RF system is determined by the radiation loss per turn:

$$\begin{aligned} U &= c_\gamma \cdot \frac{E^4}{\rho_0}\{1 + \frac{L_{ID}\cdot\rho_0}{4\pi\rho_{wi}^2}\} \\ &= U_{Bend} + U_{Wiggler} \qquad (4.5.14) \\ &= 529.4\,KeV + 3422\,KeV = 3.95\,MeV \end{aligned}$$

The energy acceptance $[\frac{\Delta E}{E}]_{RF}$ of the RF system should be about ten times the energy spread, i.e. around 2 %. It is given by

$$\frac{\Delta E}{E}_{RF} = \sqrt{k^\star} \cdot \sqrt{F(q)} \qquad (4.5.15)$$

with

$$k^\star = \frac{U}{\pi \cdot \alpha \cdot h \cdot E_0} \qquad (4.5.16)$$

and

$$F(q) = 2\{\sqrt{q^2 - 1} - \cos^{-1}(1/q)\} \qquad (4.5.17)$$

With an over-voltage factor of $q = 1.10$ to 2.0 the energy acceptance is from 1.15 % to 5.70 %, which is just in the proper range. For the layout of the RF-system one has to bear in mind, that the over voltage factor q influences the bunch length, too. A high q value leads to a small bunch length, hence also from this point of view the over-voltage factor can be used for choosing the right bunch length.

The klystron has to deliver the following power:

$$\begin{aligned} P_{Klyst} &= P_{CAV} + P_{Beam} + P_{Refl} + P_{HOM} \qquad (4.5.18) \\ & \qquad (4.5.19) \\ &\approx 1.2(P_{CAV} + P_{Beam} + P_{Refl}) \qquad (4.5.20) \end{aligned}$$

With $P_{\mathrm{refl}} = 0$ the coupling factor becomes

$$\beta_{opt} = \frac{P_{Beam}}{P_{CAV}} + 1 \qquad (4.5.21)$$

and with $P_{\mathrm{in}} = P_{\mathrm{Beam}} + P_{\mathrm{CAV}}$ it follows

$$P_{CAV} = \frac{P_{in}}{\beta} \; and \; P_{Beam} = \frac{\beta - 1}{\beta} \cdot P_{in} \tag{4.5.22}$$

By taking an over voltage factor of 2.0 the necessary overall installation of the cavity voltage is 7.9 MV with a beam power P_{Beam} of 1.2 MW.

The number of cavities is determined by the power which can be fed through the input coupler. For the ELETTRA normal conducting cavity [18] as well as the HERA superconducting one [23] it is around 110 kW. Hence overall 10 to 12 cavities have to be installed. The CESR - superconducting cavity [30],[31] is designed for an input power up to 250 kW. Already achieved have been 150 kW. This means that 5 to 8 cavities have to be installed. The specification of the CESR - cavity are: G = 6 MV/m, V_{RF} = 1.8 MV, $Q_0 = 1 \cdot 10^9$, (R/Q = 89 Ω/cell, $Q_L = 2 \cdot 10^5$ and l_{eff} = 0.3 m). Taking 5 cavities with a gradient of 1.8 MV/cell the overall RF voltage leads to q = 2.6, with an RF energy acceptance of 7.2 %.

By taking an over-voltage factor of q = 2.60 and the phase ϕ_s = 22.62 degrees, the synchrotron tune results in

$$\begin{aligned} \nu_s &= \frac{\Omega_s}{\omega_0} = \sqrt{\frac{\alpha \cdot \; h \cdot \cos\phi_s}{2\pi} \cdot \frac{eV_{RF}}{E_0}} \\ \nu_s &= \sqrt{7.96 \cdot 10^{-5}} = 8.92 \cdot 10^{-3} \\ \Omega_s &= \nu_s \cdot \omega_0 = \nu_s \cdot \frac{2 \cdot \pi}{h \cdot T_{RF}} = 2.55 \cdot 10^4 \\ f_s &= 9.724 \; KHz \end{aligned} \tag{4.5.23}$$

The bunch length is then, with $\frac{\sigma_E}{E} = 2.2 \cdot 10^{-3}$

$$\sigma_z = \frac{\alpha \cdot c}{\Omega_s}(\sigma_s/E) = 4.25 \; mm \tag{4.5.24}$$

4.5.6 Instabilities

4.5.6.1 Single Bunch Instabilities

The microwave instability, sometimes referred to as turbulent bunch lengthening, causes an increase in both the momentum spread and the bunch length of a bunched beam. The threshold (peak) current I_p is given by [23]

$$I_p^{th} = \frac{2 \cdot \pi \cdot \alpha \cdot (E/e)}{[Z_L/n]} \cdot (\sigma_E/E)^2 \tag{4.5.25}$$

$[Z_L/n]$ is the broad band impedance of the storage ring. With

$$I_p^{th} = \frac{N_E \cdot e \cdot c}{\sqrt{2\pi} \cdot \sigma_z} \tag{4.5.26}$$

and the average current I_{aver} of one bunch

$$I_{aver} = \frac{N_E \cdot e \cdot c}{2\pi \cdot R} \tag{4.5.27}$$

we get:

$$I_{aver} = \frac{\sqrt{2\pi} \cdot \alpha \cdot (E/e)}{Z_L/n} \cdot \frac{\sigma_z}{R} \cdot (\sigma_E/E)^2 \tag{4.5.28}$$

With $I_{aver} = 0.8$ mA, $\alpha = 1.64 \cdot 10^{-4}$, $\sigma_z = 4 \cdot 10^{-3}$ m, $(\sigma_E/E) = 2.2 \cdot 10^{-3}$ and R = 104 m one gets for the broad band impedance a maximum value of $[Z_L/n] = 0.3\,\Omega$. The broad band impedance is given by the vacuum chamber and the cavities:

$$[Z_L/n] = [Z_L/n]_{chamb.} + N_{CAV} \cdot [Z_L/n]_{CAV} \tag{4.5.29}$$

At the synchrotron light source ELETTRA a broad band impedance of $[Z_L/n] =$ 0.75 has been measured [24],[25],[26]. It is assumed by some estimations that the contribution of the four cavities is $0.6\,\Omega$, hence the vacuum chamber has an impedance of $0.15\,\Omega$. We assume a similar value here, too. From the measured loss factor of the CESR superconducting cavity a broad band impedance of 0.03-0.05 Ω could be determined [30],[31]. With 8 cavities the contribution of the RF-system to the broad band impedance is 0.24-0.4 Ω. From this we can estimate the impedance as:

$$[Z_L/n] = (0.4 - 0.7)\ \Omega \tag{4.5.30}$$

which is about a factor of two larger than desirable. However, by taking into account the Spear scaling rule:

$$[Z_L/n]_{eff} = [Z_L/n]_0 \cdot (\frac{\sigma_l}{b})^{1.68} = 0.70 \cdot (\frac{4.5}{20})^{1.68} = 0.06\ \Omega \tag{4.5.31}$$

the effective impedance appears to be below the allowed value. So bunch lengthening seems to be avoidable, but not with a large safety margin and further studies of this issue are required.

4.5.6.2 Multibunch Instabilities

With 333 stored bunches and a total current of 300 mA, multibunch instabilities are of concern. In this case the frequency of a Fourier component of the beam current is in resonance with a higher order mode of the cavities. The resonance conditions for the longitudinal direction is:

$$f_{cbn} = (p \cdot h + N_{cbn} + Q_s) \cdot f_0 \tag{4.5.32}$$

f_0 = revolution frequency, N_{cbn} = coupled bunch number, h = number of bunches, Q_s = synchrotron tune and p is an integer. The distance between coupled bunch mode frequencies is equal the revolution frequency f_0, which has for the DR a value of 454.5 kHz.

The higher order mode frequency f_{HOM} is a function of the dimensions of each cavity (for each cavity the f_{HOM}'s can be slightly different) and furthermore (for conventional cavities) the frequency depends upon the cavity temperature [27],[28],[29].

The growth rate for the longitudinal coupling bunch instability is

$$\frac{1}{\tau_{||}} = \frac{\alpha \cdot I_b \cdot f_0}{2 \cdot f_s \cdot (E/e)} \cdot f_{cbn} \cdot R_{S,||} \tag{4.5.33}$$

I_b is the total current within the ring and $R_{S,||}$ is the shunt impedance of the corresponding HOM. Stability is guaranteed if

$$\frac{1}{\tau_{||}} < \frac{1}{\tau_\varepsilon} \tag{4.5.34}$$

where $1/\tau_\varepsilon$ is the damping rate of the synchrotron oscillations. Taking a shunt impedance of $R_{S,||} = 200\ k\Omega$ (which is typical for a normal conducting cavity) results in a maximum current of 136 mA.

The shunt impedances of the HOM's within a CESR- superconducting cavity are in the range of 0.1 - 0.7 kΩ, leading to an instability threshold of I $\geq$ 380 mA. Hence the coupled bunch instabilities are of no importance when using superconducting cavities.

As in the longitudinal direction there are coupled bunch instabilities in the transverse direction, too. For a transverse impedance of $R_\perp = 11\ M\Omega/m$ (which is typical for a normal conducting cavity) the maximum stored beam within the DR is 4.0 mA. The transverse impedances of the CESR-SC-cavity are smaller than 0.025 MΩ/m leading to a threshold current of 1760 mA. In this case, however, other contributions to the impedance (in particular the resistive wall impedance) may become dominant. Whether or not a feedback system is required, must be determined by more detailed investigations. In any case it should be noted that the issue of multibunch instabilities is significantly relaxed compared to the B-factory rings presently under construction at SLAC and KEK.

4.5.7 Complete Ring Layout

The length of the straight section is 6 m which allows to install four cavities. For the installation of the necessary number of cavities of the RF system a total of four straight sections are needed. Accounting for one straight section each for injection and extraction, every sixth straight section must be without a damping wiggler. Thus the damping ring can be composed of six identical super-periods consisting of six unit cells, five with wigglers in the straight sections and at each side the matching sections (Fig. 4.5.9). The lattice functions within a super period are presented in Fig. 4.5.10.

To get for the full matching section (see figure 4.5.11) the same phase advance as inside the unit cell one has to introduce in the straight sections 3 quadrupoles. The one in the middle must be, according to the behaviour of the wiggler, a defocusing one. The same phase advance has to be kept in order to avoid reductions in the dynamic aperture.

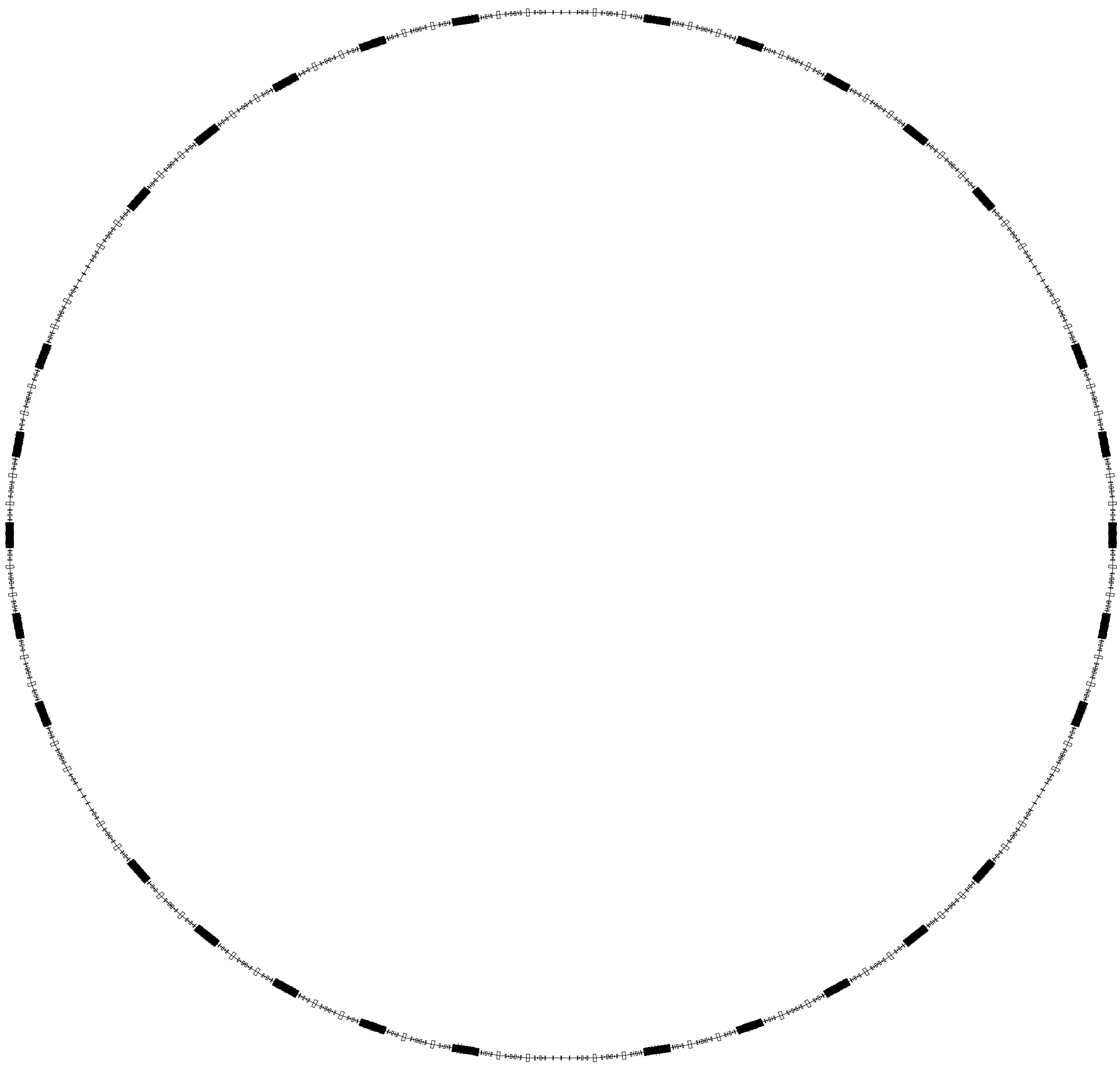

Figure 4.5.9: *Layout of the SBLC damping ring. The periodicity is six.*

The dynamic aperture, the tune shift with energy and the tune shift with particle amplitude of the damping ring with wigglers are presented in Figs. 4.5.12,4.5.13 and 4.5.14, respectively. The calculations have been done without any errors and misalignments.

According to these results the acceptances are $A_x = 145$ mm mrad and $A_y =$

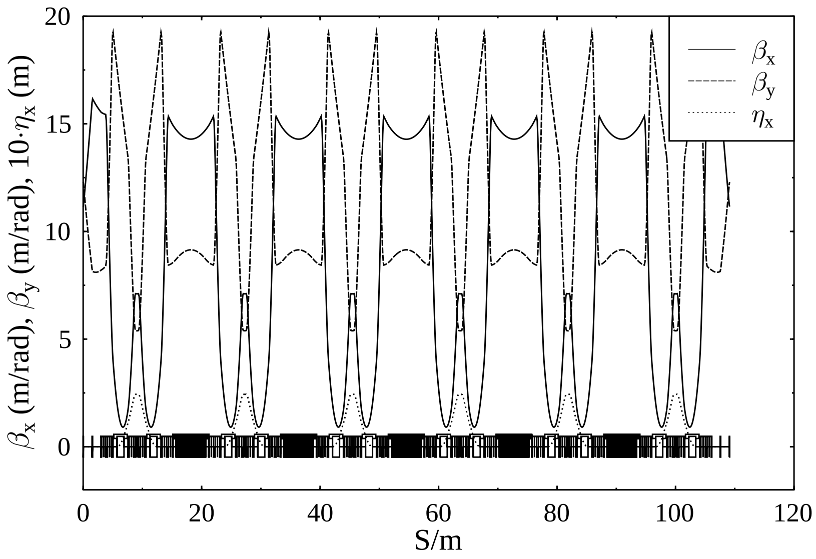

Figure 4.5.10: *Lattice functions within one super period of the SBLC damping ring. Each super period consists of the unit cells with wigglers and two matching sections at each side.*

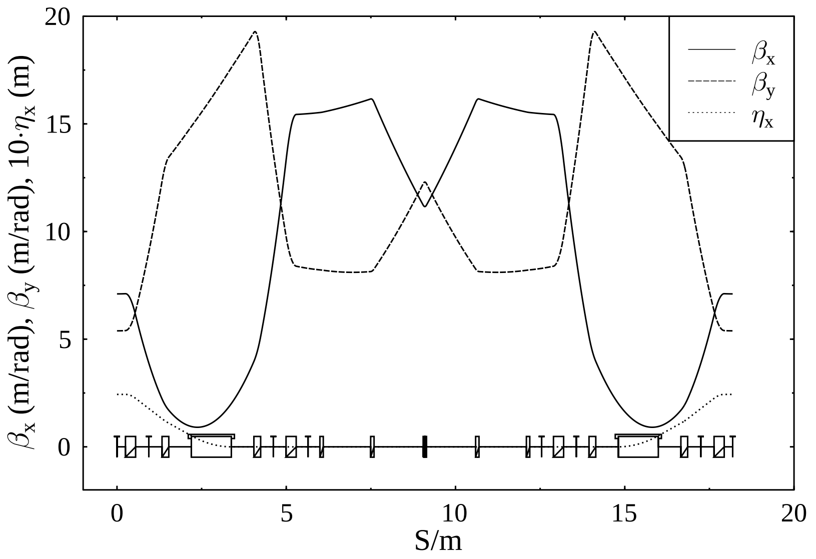

Figure 4.5.11: *Lattice functions within the matching sections of the super period of the SBLC damping ring.*

242 mm mrad, which is sufficient. The energy acceptance is larger than 3 %. The calculations of the tune shift with amplitude (see Fig. 4.5.14) are performed with a coupling of 75 % between the y- and the x- direction. Hence the maximum amplitudes according to Fig. 4.5.14 are in agreement with the dynamic aperture presented in Fig. 4.5.12.

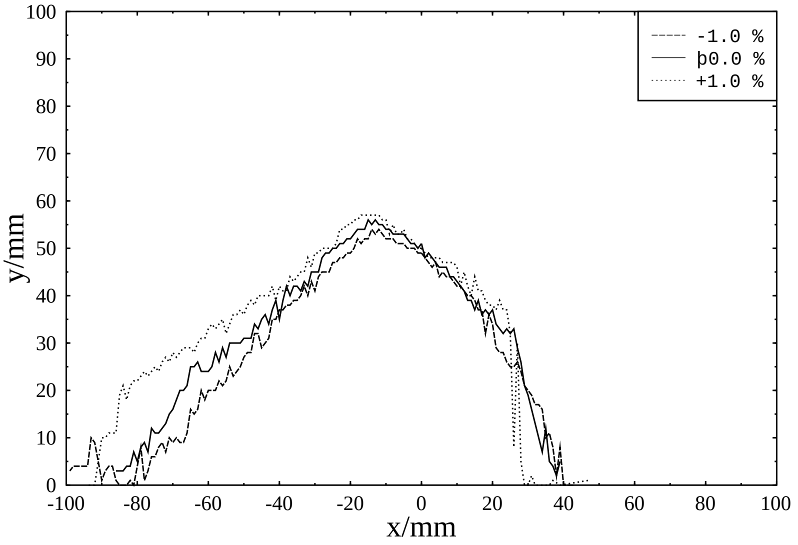

Figure 4.5.12: *Dynamic aperture of the SBLC damping ring.*

The reduction of the dynamic aperture in the presence of magnet misalignments is demonstrated in Figs. 4.5.15 and 4.5.16. The graph corresponds to normally distributed alignment errors of $\Delta_x = \Delta_y = 75\mu$m where the Gaussian distribution was truncated at 2σ.

Figure 4.5.15 includes the misalignment of bendings, quadrupoles and sextupoles, Fig. 4.5.16 shows the effect of sextupoles misalignments only. In both cases a correction of the closed orbit has not been performed.

The dynamic aperture including closed-orbit deviations due to magnetic misalignment and field errors ($\Delta B/B = 5 \cdot 10^{-3}$, $\Delta G/G = 1 \cdot 10^{-3}$) is presented in Fig. 4.5.17. Drawing an inside semi circle of the dynamic aperture the stable region would be $\Delta x \leq 35\,mm$ and $\Delta y \leq 40\,mm$ resulting in the acceptances $E_x = 108$ mm mrad and $E_y = 128$ mm mrad. For the injected positron beam with $\varepsilon_{inj}/\gamma = 1.7\text{mm} \cdot mrad$ it follows a ratio $A_x/\sigma_{x,inj} = 7.7$ and $A_y/\sigma_{y,inj} = 8.8$. For the injected electrons these radios are ten times higher. Hence the acceptance of the machine is large enough to capture the incoming particles.

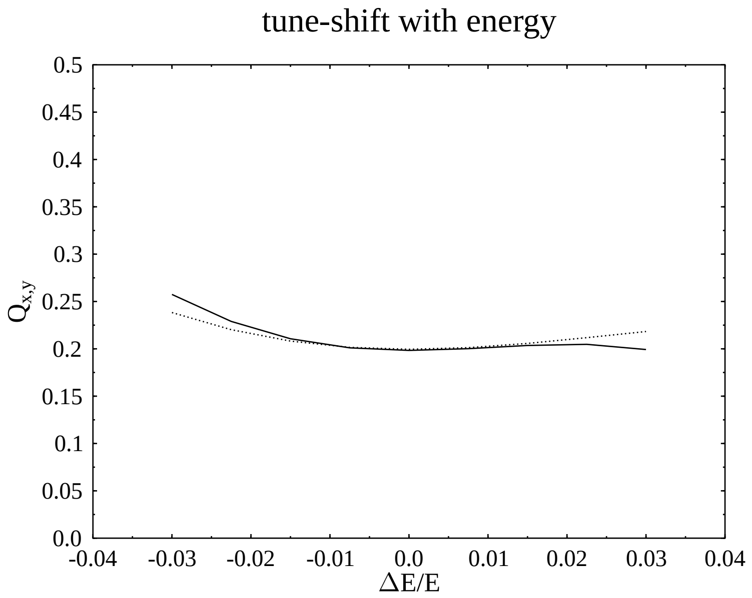

Figure 4.5.13: *Tune shift with energy of the SBLC damping ring.*

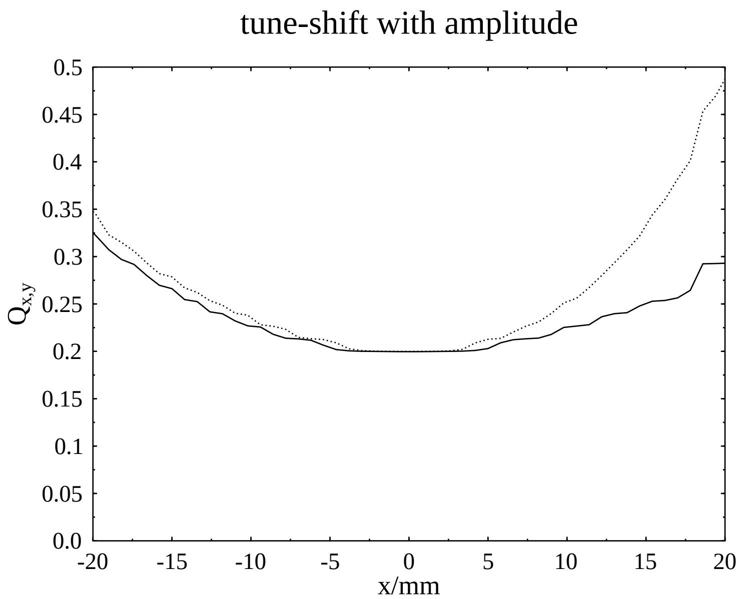

Figure 4.5.14: *Tune shift with amplitude of the SBLC damping ring at 75 % coupling, i.e* $a_y = 0.75 \cdot a_x$.

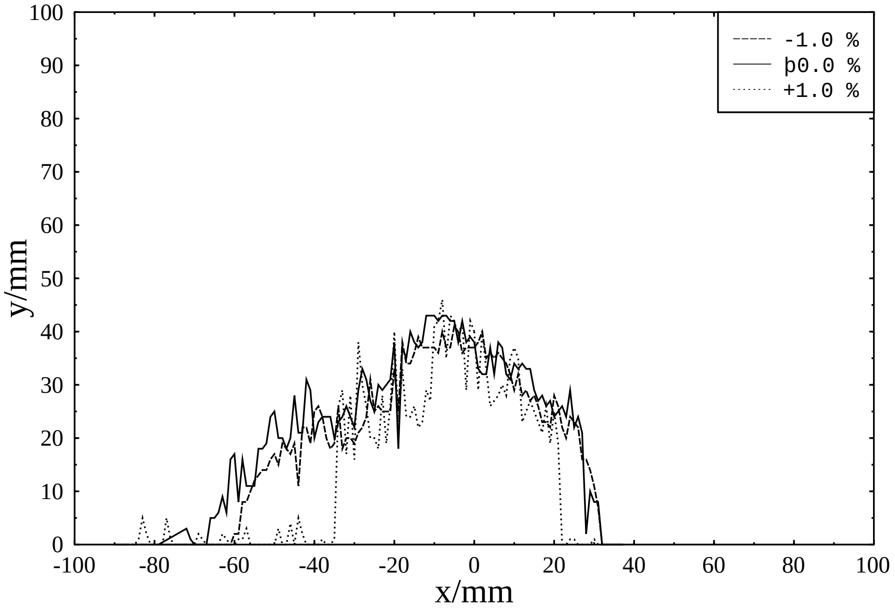

Figure 4.5.15: *The dynamic aperture of the SBLC damping ring with average alignment errors of all magnetic elements* $\Delta_x = \Delta_y = 75\mu m$.

4.5.8 Alignment Tolerances and the Vertical Emittance

The vertical equilibrium emittance is essentially determined by the magnet and beam position monitor (BPM) alignment tolerances and by the orbit correction procedures applied. We used the PETROS computer code to simulate alignment errors and orbit correction procedures. Assuming rms magnet and BPM position tolerances of $50\,\mu$m, the MICADO algorithm (a standard orbit correction method applied routinely at LEP, HERA and other storage rings) [32] is applied in several iterations until the quality of the orbit does not improve anymore. From 10 different random seeds of errors we obtain an average vertical normalized emittance of $(1.0 \pm 0.9)\cdot 10^{-7}$ m. So the required emittance could just be achieved with the assumed tolerances and standard correction techniques. Further improvements are possible by introducing dispersion correction orbit bumps and/or skew quadrupoles, and by better effective alignment of the BPM's w.r.t. to the magnets using beam-based methods.

4.5.9 Specifications of the Magnet Elements

The injected electron beam has a normalised emittance of $1 \cdot 10^{-4}$ m which leads to a maximum beam size of 0.5 mm ($1\ \sigma$). In order to get a sufficient quantum lifetime the acceptance should be a factor six to ten larger. Including closed orbit deviations of 5 mm and a thickness of the vacuum chamber of 2 mm it was chosen to have a gap in

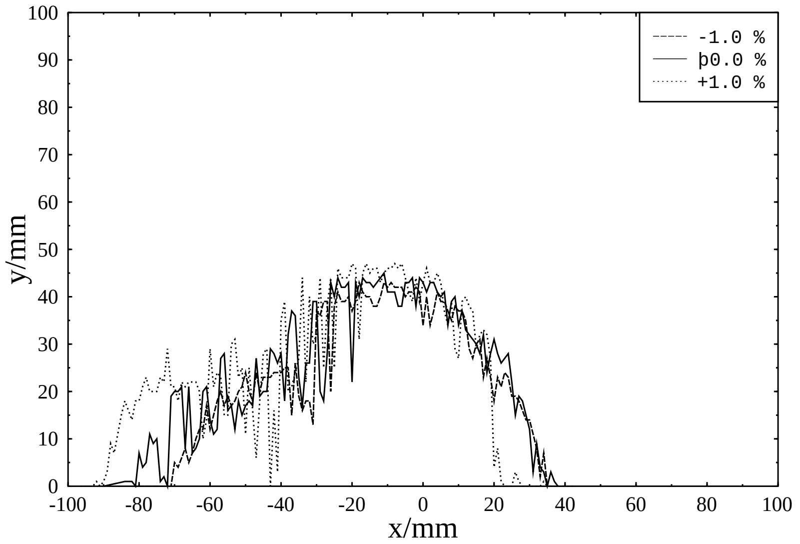

Figure 4.5.16: *Dynamic aperture of the SBLC damping ring with misaligned sextupoles* $(\Delta_x = \Delta_y = 75\mu m)$.

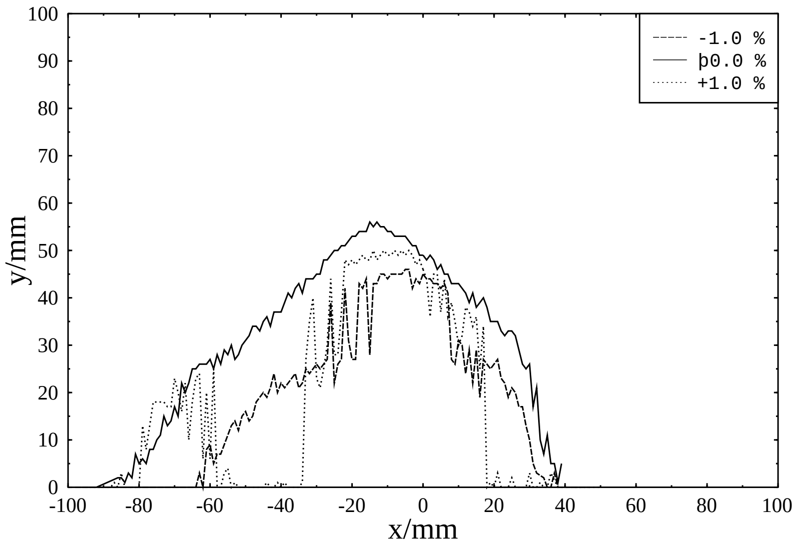

Figure 4.5.17: *Dynamic aperture of the SBLC-damping ring with field errors* $\Delta B/B = 5 \cdot 10^{-4}$ *for the bending and* $\Delta G/G = 5 \cdot 10^{-3}$ *for the quads.*

the bending magnet of ± 15 mm and a bore within the quadrupoles and sextupoles of $r_0 = 20$ mm. With a pole tip field for the quads and sextupoles of 0.6 T and 0.5 T, respectively, the maximum gradients are $g_{max} = 30$ T/m and $g'_{max} = 2500\,\mathrm{T}/m^2$. The specifications of the magnets for the electron damping ring are summarised in Table 4.5.5.

For the positrons the size (1 σ) of the injected beam will be 5 mm. A factor of 6 between the physical aperture and the cross section should be enough in order to get a sufficient lifetime, because the acceleration time is only 20 ms. The gap within the bendings was chosen to be $\pm$ 20 mm and the bores within the quadrupoles and sextupoles of $\pm$ 35 mm. Similar values have been used for 3rd generation light sources. With this diameters in the quads and sextupoles the maximum gradient decreases to:

$$g_{max} = 18\ T/m \text{ and } \mathrm{g}'_{\mathrm{max}} = 816\mathrm{T/m}^2 \tag{4.5.35}$$

The specifications of the magnets for the positron damping ring are summarised in Table 4.5.6.

Table 4.5.5: *Specification of the magnets for the electron damping ring.*

Bendings:

Energy	3 GeV
Number of magnets	72
Curvature	13.54 m
Magnetic flux	0.739 T
Gap	30 mm
Magnetic length	1.18 m
Ampere turns	23.6 kA
Number of coil windings	72
Nominal current	245

Quadrupoles:

Type	Q_A	Q_B	Q_C	Q_D	Q_E
Number	72	144	72	78	12
Magnetic length [m]	0.05	0.20	0.15	0.10	0.10
Aperture [mm]	40.0	40.0	40.0	40.0	40.0
Gradient [T/m]	1.0	25.5	28.0	28.0	13.0
Ampere turns [kA]	0.16	4.06	4.46	4.46	2.07
Number of coil windings	10	20	20	20	20
Current	16	203	223	223	103

Sextupoles:

Type	S_1	S_2	S_H	S_V
Number	72	72	36	72
Magnetic length	0.05	0.05	0.10	0.10
Aperture	40.0	40.0	40.0	40.0
Diff. gradient [T/m^2]	556	708	1810	1036
Ampere turns [kA]	0.59	0.751	1.921	1.099
Number of coil windings	20	20	30	30
Current [A]	30	37.6	64	36.6

Table 4.5.6: *Specification of the magnets for the positron damping ring.*

Bendings:

Energy	3 GeV
Number of magnets	72
Curvature	13.54 m
Magnetic flux	0.739 T
Gap	40 mm
Magnetic length	1.18 m
Ampere turns	17.5 kA
Number of coil windings	72
Nominal current	328

Quadrupoles:

Type	Q_A	Q_B	Q_C	Q_D	Q_E
Number	72	144	72	78	12
Magnetic length [m]	0.05	0.28	0.23	0.15	0.10
Aperture [mm]	70.0	70.0	70.0	70.0	70.0
Gradient [T/m]	1.0	18.0	18.0	18.0	13.0
Ampere turns [kA]	0.49	8.77	8.77	8.77	8.77
Number of coil windings	10	30	30	30	30
Current	49	292	292	292	211

Sextupole:

Type	S_1	S_2	S_H	S_V
Number	72	72	36	72
Magnetic length	0.05	0.05	0.25	0.15
Aperture	70.0	70.0	70.0	70.0
Diff. gradient [T/m^2]	556	708	724	691
Ampere turns [kA]	3.164	4.026	4.117	3.929
Number of coil windings	20	20	20	20
Current [A]	158	201	206	196

Bibliography

[1] R. Brinkmann, *A Study of Low - Emittance damping ring Lattices*, DESY M-90-09, July 1990

[2] ATF, Accelerator Test facility, Design and Study Report, Internal Report 95-4, June 1995

[3] NCL damping ring, Zeroth-Order Design Report for the next Linear Collider, SLAC, Stanford, 1996.

[4] A. von Steenberger, *Collider Damping Ring, Theoretical Minimum Emittance Structure*, Proceedings of the ICFA Workshop on Low Emittance $e^- - e^+$ Beams, BNL (1987), p.60.

[5] H.Z. Zyngier et. al., *VUV Radiation Source Super ACO*, IEEE Trans. on Nucl. NS-32, 3371 (1985).

[6] D. Einfeld and M. Plesko, *A modified QBA optics for low emittance storage rings*, NIM A335 (1993) 402-416.

[7] D.Einfeld, J.Schaper, M.Plesko, *Design of a Diffraction limited Light Source*, SPIE 2013 (1993) 201-212.

[8] D. Einfeld et al., *The synchrotron light source ROSY*, NIM B89 (1994) 74-78

[9] D. Einfeld et al., *Design of a SBLC-Damping ring with a TBA-optics*, to be published.

[10] 1-2 GeV synchrotron Radiation Sources, PUB-5172 Rev., July 86, LBL, California 94720.

[11] ESRF Foundation Phase Report, February 1987, European Synchrotron Radiation Facility, B.P.220-38043, Grenoble Cedex.

[12] 10th ICFA Beam Dynamics Panel Workshop, 4th Generation Light Sources, Grenoble 1996.

[13] J. Murphy, *Synchrotron Light Source DATA Book*, BNL/NSLS, BNL 42333, Version 4.

[14] A.Ropert, *High Brilliance Lattices and the Effect of Insertion Devices*, CAS: Synchrotron Radiation and Free Electron Laser, CERN 90-03, April 1990.

[15] R.P. Walker, *Wigglers*, Fifth Advanced Accelerator Physics Course, CERN 95-06, Vol.II, November 1995.

[16] D.Einfeld, J.Schaper, M.Plesko, *Design of a Diffraction limited Light Source*, WG3-53, see [7]

[17] A.Wrulich, *Overview of 3rd Generation Light Sources, Workshop on Forth Generation Light sources*, February 24-27, 1992, SSRL 92/02.

[18] ELETTRA, Conceptional Design Report, Sincrotrone Trieste, Padriciano 99, I-34012 Italy.

[19] H.Grote and F.C.Iselin, *The MAD Program,Version 8.16*, CERN/SL/90-13 (AP), 1995.

[20] F.Iazzourene,C.J.Bocchetta,R.Nagaoka,L.Tosi and A.Wrulich, RACETRACK USER'S GUIDE, Version 4.01, ST-IM-92/I ,July 1992.

[21] L.Farvaque,J.L.Laclare and A.Ropert, *BETA USER'S GUIDE*, ESRF-SR/LAT 88-08, 1988.

[22] R.Byrns, B. Dwersteg et al., *Status of the Superconducting Cavity Program for HERA*, Proceedings EPAC 90, Nice June 12-16, 1996.

[23] M.S.Zisman,S.Chattopadhyay and J.J.Bisognano, *ZAP USER'S MANUAL*, LBL-21230,December 1986.

[24] A.Wrulich,private communication.

[25] J.E.Karantzontis, *An Overview on Impedances and Impedance Measuring Methods for Accelerators*, ST/M-91/1, January 1991, Sincrotrone Trieste.

[26] J.E.Karantzontis, *The Coupling Impedance of the ELETTRA Storage Ring ST/M-TN-90/14*, August 1990, Sincrotrone Trieste.

[27] M.Svandrlik, A.Fabris, C.Pasoni, *Improved Methods of Measuring and Curing Multibunch Instabilities in ELETTRA*, Proceedings of the EPAC 96, Sitges, Spain.

[28] J.E.Karantzontis et.al., *Beam Lifetime Measurement in ELETTRA*, Proceedings of the EPAC 96, Sitges, Spain.

[29] M.Svandrlik et al., *The Cure of Multibunch instability in ELETTRA*, Proceedings of the PAC 95, Dallas, Texas, USA

[30] S.Belomestny et al, *Comparison of the Predicted and Measured Loss Factor of the Superconducting Cavity Assembly for the CESR Upgrade*, Proceedings of the PAC 95, Dallas, Texas, USA.

[31] S.Belomestnyk et al., *Wakefield and HOMs Studies of a Superconducting Cavity Mode with the CESR Beam*, Proceedings of the PAC 95, Dallas, Texas, USA

[32] B. Autin and Y. Marti, *Closed Orbit Correction in A.G. Machines Using a Small Number of Magnets*, CERN-ISR-MA-73-17, 1973.